applied sciences

MDPI

Article

Computational Shape Design Optimization of Femoral Implants: Towards Efficient Forging Manufacturing

Víctor Tuninetti [1,*], Geovanni Fuentes [1], Angelo Oñate [2], Sunny Narayan [3], Diego Celentano [4], Claudio García-Herrera [5], Brahim Menacer [6], Gonzalo Pincheira [7], César Garrido [8] and Rodrigo Valle [9,†]

1 Department of Mechanical Engineering, Universidad de La Frontera, Temuco 4811230, Chile; g.fuentes08@ufromail.cl
2 Department of Materials Engineering (DIMAT), Faculty of Engineering, Universidad de Concepción, Concepción 4070138, Chile; aonates@udec.cl
3 Department of Mechanics and Advanced Materials, Campus Monterrey, School of Engineering and Sciences, Tecnológico de Monterrey, Av. Eugenio Garza Sada 2501 Sur, Tecnológico, Monterrey 64849, NL, Mexico; s.narayan@tec.mx
4 Departamento de Ingeniería Mecánica y Metalúrgica, Pontificia Universidad Católica de Chile, Principal Investigator of the MIGA Millennium Institute (ICN2021_023), Av. Vicuña Mackenna 4860, Santiago 7820436, Chile; dcelentano@uc.cl
5 Departamento de Ingeniería Mecánica, Universidad de Santiago de Chile (USACH), Av. Bernardo O'Higgins 3363, Santiago 9170016, Chile; claudio.garcia@usach.cl
6 Laboratoire des Systèmes Complexe (LSC), Ecole Supérieure en Génie Electrique et Energétique ESGEE Oran, Chemin Vicinal N9, Oran 31000, Algeria; menacer_brahim@esgee-oran.dz
7 Department of Industrial Technologies, Faculty of Engineering, University of Talca, Camino a Los Niches Km 1, Curicó 3344158, Chile; gpincheira@utalca.cl
8 Department of Mechanical Engineering, Universidad del Bío-Bío, Concepción 4081112, Chile; cgarrido@ubiobio.cl
9 Faculty of Engineering, University of Talca, Camino a Los Niches Km 1, Curicó 3344158, Chile; rodrigo.valle@uautonoma.cl or r.vallefuentes@gmail.com
* Correspondence: victor.tuninetti@ufrontera.cl
† Current address: Facultad de Arquitectura, Construcción y Medio Ambiente, Universidad Autónoma de Chile, Talca 3460000, Chile.

check for updates

Citation: Tuninetti, V.; Fuentes, G.; Oñate, A.; Narayan, S.; Celentano, D.; García-Herrera, C.; Menacer, B.; Pincheira, G.; Garrido, C.; Valle, R. Computational Shape Design Optimization of Femoral Implants: Towards Efficient Forging Manufacturing. *Appl. Sci.* **2024**, *14*, 8289. https://doi.org/10.3390/app14188289

Academic Editor: Roger Narayan

Received: 19 August 2024
Revised: 7 September 2024
Accepted: 12 September 2024
Published: 14 September 2024

Abstract: Total hip replacement is one of the most successful orthopedic operations in modern times. Osteolysis of the femur bone results in implant loosening and failure due to improper loading. To reduce induced stress, enhance load transfer, and minimize stress, the use of Ti-6Al-4V alloy in bone implants was investigated. The objective of this study was to perform a three-dimensional finite element analysis (FEA) of the femoral stem to optimize its shape and analyze the developed deformations and stresses under operational loads. In addition, the challenges associated with the manufacturing optimization of the femoral stem using large strain-based finite element modeling were addressed. The numerical findings showed that the optimized femoral stem using Ti-6Al-4V alloy under the normal daily activities of a person presented a strains distribution that promote uniform load transfer from the proximal to the distal area, and provided a mass reduction of 26%. The stress distribution was found to range from 700 to 0.2 MPa in the critical neck area of the implant. The developed computational tool allows for improved customized designs that lower the risk of prosthesis loss due to stress shielding.

Keywords: hip replacement; femoral stem; bone implant; finite element analysis; topological optimization

1. Introduction and General Background

The healthcare industry is constantly seeking new materials and techniques to provide better treatments for patients and improve their quality of life. In recent years, titanium alloys have replaced cobalt–chromium alloys and stainless steel in the manufacture of

mechanical implant devices. This shift has generated greater interest in titanium and its alloys and expanded their range of applications.

Hip prostheses are mechanical implants designed to replace damaged hip joints, playing a critical role in restoring joint function and improving the quality of life for patients. These implants must allow proper joint movement, stabilize the articulation, and support the body's weight. The primary goal of hip arthroplasty is to achieve a pain-free, highly mobile joint with sufficient surrounding muscle quality to facilitate natural movement. There are various types of hip prostheses available, including total, partial, and resurfacing implants, which can be fixed to the bone using cemented, cementless, or hybrid fixation methods. A proper surgical technique is crucial for ensuring successful long-term implant fixation and integration. Cemented hip prostheses involve injecting bone cement to create a durable interface [1], while uncemented implants rely on a porous or coated surface to promote stability and bone ingrowth, a process that takes longer to fully achieve [2]. Femoral implants in particular can utilize a range of surface coatings that are categorized by their roughness scale; this includes macroscale, microscale, and nanoscale treatments, which have been shown to significantly impact the bone–implant integration process [3,4].

Titanium and its alloys have emerged as the material of choice for biomedical applications, particularly in the design of orthopedic implants, due to their superior corrosion resistance, biocompatibility, and mechanical properties [5]. Among the various titanium alloys, low-modulus β-type titanium alloys have gained significant attention in recent years as they address the critical issue of stress shielding, which is a common problem associated with traditional titanium alloy implants [6]. In particular, Ti-6Al-4V, known as grade 5 titanium, has proven to be highly compatible with the human body for use in prostheses and orthopedic implants. This alloy has a low density, high hardness, and, most importantly for these applications, high biocompatibility. This material is known for its bioinert quality, which ensures a stable chemical response when in contact with tissues or living cells. This reduces the likelihood of the body rejecting it. Its combination of strength, light weight and corrosion resistance makes this an ideal material for use in a variety of applications, including the aerospace, automotive and medical industries. Furthermore, it is reported as a material that has adequate osseointegration, which is required not only for the correct regeneration of the bone around the prosthesis in the early phases, but also to ensure its stable long-term use.

The design and simulation of hip joint prostheses using finite-element-based computational tools for analyzing the complex biomechanical interactions and performance of orthopedic implants has been applied to validate the feasibility of materials such as Ti-6Al-4V and TiNbZrTaFe alloy [7], and even fiber-reinforced polymer composites (CFRPCs) [8]. This has been of continuous interest in biomedical engineering design because achieving maximum load during walking in simulated conditions and using reduced implant material with accurate performance requires the advanced modeling of the implant assembly and the realistic application of forces, moments, and stress projections of the femur model [9]. A low-stiffness porous Ti6Al4V hip prosthesis has been developed by Naghavi et al. [10] via selective laser melting (SLM) to minimize stress variations following hip replacement. The study demonstrates a potential reduction in stress shielding by 70% and bone mass loss by 60%, suggesting a viable alternative to the generic solid implant. The study presented by Johnson et al. [11] evaluates mechanical behavior under idealized and physiological loading conditions to compare the femoral fracture risk classifications with metastatic bone disease using different finite element simulation approaches, demonstrating that the incorporation of physiological muscle forces significantly affects local deformation. The strategy based on topological optimization in hip prostheses allows a reduction in stress shielding, an increase in the strength-to-weight ratio and an improvement in dynamic behavior, which leads to greater implant durability due to a reduction in aseptic loosening [12].

Optimization algorithms allow the best bone–implant stability to be determined [13]. In the study Tan et al. [14], a martensitic TiNi biomaterial with a low modulus and mechanical behavior mimicking human bones is studied. The bioinspired structure exhibits both strength and ductility. Additionally, it is shown that post-processing heat treatments alter the microstructure, resulting in a hierarchically reinforced multiscale behavior, offering one of the highest specific strengths (around 70 kN m/kg) among porous biomaterials. Ceddia et al. [15] analyzed the criticalities in the contact between the femoral head and the stem neck, showing that in proximal contact, the stress levels can exceed 500 MPa in certain areas of the prosthesis. Meena et al. [16] studied the changes in stress distribution in the femur after total hip replacement by providing simulated in vivo loading and boundary conditions. The loading and boundary conditions were generated using the musculoskeletal modelling software 'AnyBody'. The results showed considerable variations in the stress distribution pattern in the femur before and after total hip replacement, with the metallic implant taking major loads and transferring very little load to the femur. Oza et al. [17] investigated the stress–strain and force displacement at the bone–implant interface using the finite element analysis of implant models. This study demonstrated that the maximum principal stress generated in the solid hip stem, both with and without the femoral bone, remains below the safe limit, exhibiting good mechanical properties and strength. Kebbach et al. [18] showed that a musculoskeletal multibody simulation framework was capable of virtually characterizing the knee joint dynamics for different TKR designs. Xiao et al. [19] proposed a parallel optimization method to study the topological structure of a type A femoral stem. Kan et al. [20] compared a rational inner scaffold and the topology optimization design of an implant by considering the clinical design requirements, patient customization, weight reduction, and mechanical stability. Sun et al. [21] provided a comprehensive overview of the modelling procedures for predicting the aseptic loosening risk, focusing on cementless femoral stems. A femur fixed with different osteosynthesis plates was simulated using the finite element technique and a statistical analysis of a region of interest placed in the femur diaphysis showed that the biomechanical effect of using the dual plate system was smaller in the osteotomy region than at the femur head [22].

Implant stress, bone atrophy and loosening are related to the use of a material with a Young's modulus much higher than that of cortical bone. This failure of a joint is known as stress shielding, and to mitigate this effect, the adequate design optimization of hip prostheses is required. Stress shielding occurs when the alloy inserted into the bone has a different elastic modulus, and therefore, the stresses are not uniformly distributed over the bone–implant interface; regions of stress concentration can then lead to inflammation in the bone, reducing its ability to remodel. For example, the Ti6Al4V alloy exhibits a Young's modulus of 109 Gpa, between four to ten times that of cortical bone (10–30 GPa). In addition, the implant exerting excessive local stress on the bone may even lead to bone atrophy and the consequent loosening of the implant. Such findings have important implications for implant design and material selection, as the relationship between material properties and bone properties must be taken into account to avoid complications. Therefore, further research in this field is needed to improve the efficacy and safety of implants in the treatment of various medical conditions.

While the geometric design of custom femoral implants is critical for their long-term success, current design approaches often result in inhomogeneous stress distributions, suggesting a lack of full optimization. Addressing this gap, this work introduces a novel finite element simulation strategy for optimizing custom femoral implant design. The geometric design of this implant is widely recognized as a critical factor in determining the long-term success and performance of the implant, as it can significantly impact the stress distribution within the implant and the surrounding bone. Several studies have reported the presence of an inhomogeneous stress field within the implant, suggesting that the current design approaches may not be fully optimized. Finite element modeling provides a valuable computational platform to analyze these complex biomechanical interactions between the implant and the surrounding bone, and to identify specific design

modifications that can effectively mitigate stress concentrations and improve the overall biomechanical compatibility. By optimizing the geometric features of the femoral implant, such as the shape, dimensions, surface textures, and material composition, the mismatch in elastic modulus between the implant and the surrounding bone can be minimized, thereby reducing the risk of stress shielding and subsequent bone resorption. In this study, the critical design challenge addressed with the three-dimensional finite element analysis (FEA) of a femoral stem is the shape optimization, by analyzing the developed deformations and stresses under operational loads. Overall, the novel systematic optimization approach and computational tool presented target the enhancement of the long-term stability, integration, and functional performance of prosthetic systems.

2. Materials and Methods

2.1. Titanium Alloys

In this work, the femoral implant is designed and manufacturing is investigated using Ti-6Al-4V. Ti-6Al-4V is one of the most used materials in the manufacture of implants. Its low density, high hardness, high corrosion resistance and excellent biocompatibility make it a real option for biological applications. When comparing Ti with other biocompatible metals such as stainless steel and the Co-Cr alloy, we found that titanium has a much lower density, being 4.7 g/cm; that of stainless steel is 7.9 g/cm and that of the CoCrMo and CoNiCrMo alloys is 8.3 g/cm and 9.2 g/cm, respectively. Titanium exhibits mechanical properties similar to those of these metals and a higher resistance to corrosion. This Ti metal and its alloys are very difficult to work cold, so it is usually forged hot, at a temperature close to 800 °C.

Both titanium and its alloys have a Young's modulus of around 110 GPa. This value is practically half that of other metals such as stainless steel or the Co-Cr alloy, which is why titanium is the metal most elastically compatible with human bone. Regarding the mechanical properties of this metal, it is observed that both the elastic limit and the tensile strength are above that of stainless steel and Co-Cr alloy. Even though some authors provide warnings regarding the biocompatibility of vanadium in the literature, there is no study that shows that this element can be harmful when it is combined in the Ti-6Al-4V alloy.

Ti-6Al-7Nb alloy emerged as a commercially available alternative to Ti-6Al-4V due to concerns about the potential carcinogenicity of vanadium. As Ti-6Al-7Nb exhibits mechanical properties similar to Ti-6Al-4V [23], its biocompatibility and stress distribution characteristics should not differ in the proposed design. However, it is essential to conduct dedicated simulations to accurately assess the performance of Ti-6Al-7Nb implants with specific identified properties and assess the model constants of the raw material.

2.2. Three-Dimensional Design of the Femoral Stem

2.2.1. Three-Dimensional Geometry

The selection of a commercial hip femoral stem that adapts to the patients' expectations was carried out. This is a design approved in the market, as it works with a template that presents the ideal measurements and thus helps to create an appropriate prosthesis for the restoration of the length of the leg and its biomedical function.

To create this three-dimensional geometry of the femoral hip stem, SolidWorks 2020 software was used (Figure 1). This stem was generated with respect to the average measurements of a common hip prosthesis. The investigated geometry and proposed optimized solution, while not directly focused on anatomical design, have the potential to be integrated with patient-specific approaches. This integration could lead to a new generation of hip implants that are both anatomically matched and biomechanically optimized, ultimately improving patient outcomes.

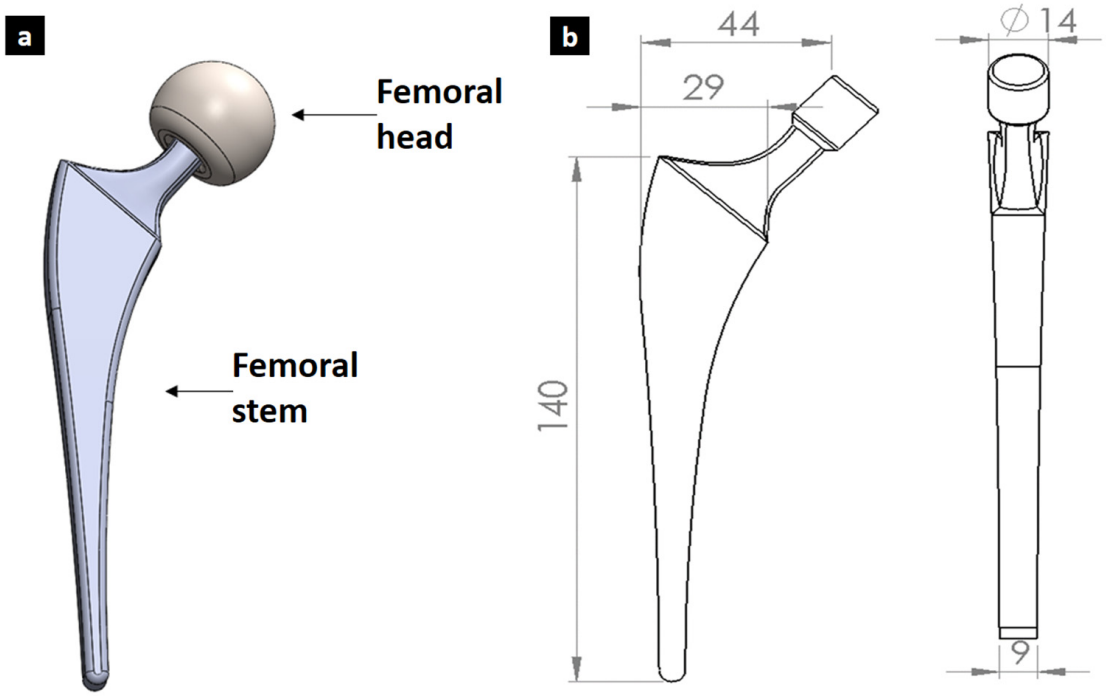

Figure 1. Initial design of femoral implant designed showing (**a**) assembly and (**b**) geometry with dimensions in mm.

2.2.2. Mechanical Models of Ti6Al4V: Model Constants and Physical Properties

The Ti-6Al-4V titanium alloy physical properties used in the simulation are the values shown in Table 1, highlighting a low density and low Young's Modulus; it is therefore an optimal material for applications that require high material resistance, a low weight and large elasticity. The material model parameters of the Johnson–Cook law of plasticity and damage are given in Tables 2 and 3. This model is applied in large deformation simulations such as forging, while for the operational loading behavior of the femur implant, Hook's law is employed to assess the elastic behavior.

Table 1. Physical properties of the Ti-6Al-4V alloy.

Properties	Value
Density (kg/m^3)	4430
Melting temperature (°C)	1605
Heat capacity (J°C/kg)	611
Modulus of elasticity (GPa)	109
Poisson's ratio (-)	0.34

Table 2. Johnson–Cook plasticity law parameters [24,25].

Parameters	Value
A (MPa)	927
B (MPa)	877.96
C (-)	0.0137
m (-)	0.594
n (-)	0.795

Table 3. Johnson–Cook model constants of the plastic deformation model at the onset of damage until fracture [26,27].

Parameters	Value
d_1	0.246
d_2	186.0
d_3	−15.7
d_4	0.2582
d_5	1.2059

The Johnson–Cook model of plasticity describes the equivalent stress ($\overline{\sigma}$) (Equation (1)) of the material as a function of the equivalent plastic strain ($\bar{\varepsilon}$), the equivalent plastic strain rate ($\dot{\bar{\varepsilon}}$), and the homologous temperature ($T^* = \left(T - T_{ref}\right) / \left(T_{melt} - T_{ref}\right)$).

$$\overline{\sigma} = (A + B \cdot \bar{\varepsilon}^n)\left[1 + C \cdot ln\left(\frac{\dot{\bar{\varepsilon}}}{\dot{\bar{\varepsilon}}_{ref}}\right)\right]\left(1 - T^{*m}\right) \quad (1)$$

The term A corresponds to the elastic limit at a reference temperature $\left(T_{ref}\right)$ and reference strain rate $\left(\dot{\bar{\varepsilon}}_{ref}\right)$. The strain hardening coefficient B and exponent n describe the reference stress–strain curve, while C identifies the material's strain rate sensitivity. The thermal softening is described by the m exponent. T is the temperature of the material, and T_{fusin} is the melting temperature of the material. If the failure of the material depends on the strain rate and temperature of the material, the Johnson–Cook failure model can be used. This expression is given by Equation (2):

$$\varepsilon_f = \left[d_1 + d_2 \cdot e^{-d_3 \cdot \eta}\right] \cdot \left[1 + d_4 \cdot ln\left(\frac{\dot{\bar{\varepsilon}}}{\dot{\bar{\varepsilon}}_{ref}}\right)\right] \cdot (1 + d_5 T^*) \quad (2)$$

where $\eta = p/\overline{\sigma}$ is the triaxiality of the stress state, defined as the ratio of the hydrostatic pressure p over the equivalent von Mises equivalent stress $\overline{\sigma}$. The parameters d_i with $i = 1\ to\ 5$ are damage-related material constants. Fracture occurs when the damage parameter D in Equation (3) has a value equal to 1.

$$D = \int \frac{d\varepsilon}{\varepsilon_f} \quad (3)$$

2.2.3. Load Applications on Femoral Implants

To determine the critical loads that act on the femoral implant, the different movements performed by a person were analyzed; for this, the hypotheses regarding the critical load conditions in the human gait cycle were investigated. One of the most relevant hypotheses is the movement that a person makes when going up and down the stairs; in more detail, it is the load that is produced on the femur when going down a high step. This load is considered four times a person's body weight [28]. In this case, it was considered that the average body weight of a person is 800 [N]; therefore, the load to be applied was 3200 [N], with a contact angle of 90° on the femoral head. This load produces slight bending in the implant. On the other hand, another critical load condition is the one generated by a person rotating the foot 90°. This effect produces torsion in the coxofemoral joint and is determined based on a multiplicative load factor. When considering the body weight of a person of 800 [N], a torsional load of 384 [N] is obtained, applied to the lateral area of the femoral head.

2.3. Mass Reduction from Shape Optimization of Femoral Stem

Once the femoral stem model was built using SolidWorks software, recognizing the loading conditions, materials and their properties, a topological optimization was carried out using the finite element method to modify the implant design. For this, the CAD model was imported into the Structural Static Analysis module of ANSYS 2020. In the Engineering Data section, the properties of grade 5 titanium for the femoral stem and femoral head were introduced. Next, the Topology Optimization module was added, in which the mesh, the loading conditions, and the restrictions presented by the stem were added.

Mesh Generation, Load Application and Boundary Conditions for Shape Optimization

For mesh generation, a tetrahedral finite element was adopted; this is commonly used to mesh complete solid models because it presents faster and more efficient meshing algorithms that better adjust to a complex geometry.

In the numerical study, the identified loading conditions on the femoral head of the implant were found to have a maximum vertical load due to the person's weight and movements of 3200 [N] producing bending and due to a lateral torsional load of 384 [N] being generated when rotating the foot 90°.

To perform the analysis of a more realistic model, the forces acting on the implant were distributed uniformly in the middle of the surface of the femoral head; considering that the total area of the femoral head is 2394 mm^2, the area selected for the loading application was 1197 mm^2. This considers two resulting pressures on the femoral head. The pressure generated when descending a large step is 2.67 [MPa], with an angle of 90° on the middle surface of the femoral head. The torsional pressure generated by turning the foot 90° is 0.32 [MPa], applied to the lateral area of the femoral head. For the analysis of the femoral implant, a combination of both critical conditions was considered (Figure 2).

Figure 2. Load distribution for shape optimization analysis.

2.4. Modelling the Full-Assembled Optimized Model of Femoral Stem

The components required for a more innovative and realistic structural analysis of the hip prosthesis are shown in Figure 3. The inside of the femoral head was designed according to the neck of the femoral stem, and the outside was designed according to the standard measurement of femoral heads in the prosthesis market (Figure 3a). The design of the cement coating was carried out according to the requirements of a cemented hip prosthesis. The cement layer to be considered was 2 mm thick and reached 1 cm below the tip of the prosthesis. The cement properties can be found in Table 4.

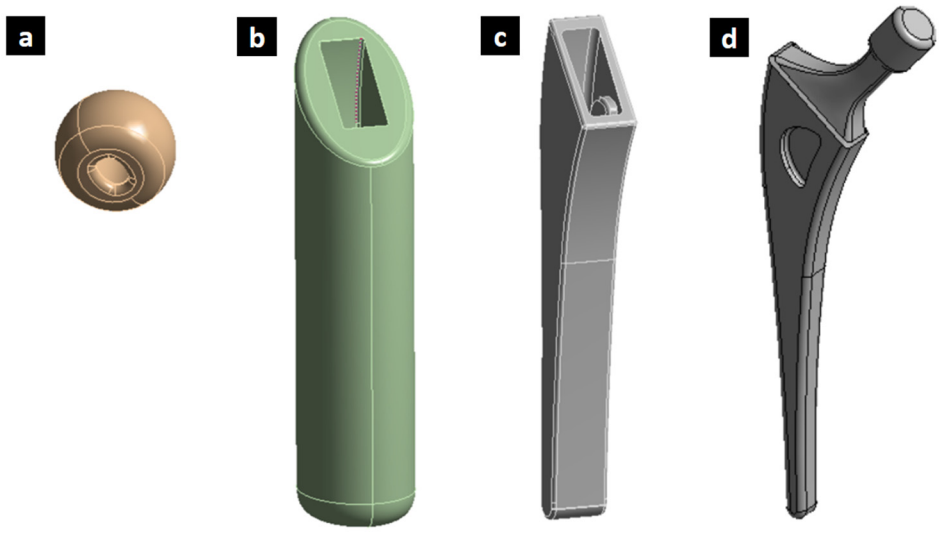

Figure 3. (**a**) Ti-6Al-4V femoral head. (**b**) Mold designed to determine the effect exerted by the cortical bone. (**c**) Cement coating of the femoral stem. (**d**) Optimized femoral implant.

Table 4. Mechanical properties of polymethylmethacrylate (PMMA) [29].

Modulus of Elasticity (GPa)	$E = 3$
Poisson	$v = 0.33$
Density (kg/m^3)	$\rho = 1200$

To determine the effect that the cortical bone exerts on the hip prosthesis, a design was created using SolidWorks, generating a bone 20 cm long and 10 cm in diameter, using the properties of the cortical bone presented in Table 5.

Table 5. Constants according to mechanical tests of a femoral bone [30].

Young's Modulus [GPa]	Shear Stiffness Modulus [GPa]	Poisson's Ratio	Density (kg/m^3)
$E_1 = 11.5$	$G_1 = 3.2$	$v_1 = 0.3$	1800
$E_2 = 17$	$G_2 = 3.6$	$v_2 = 0.45$	
$E_3 = 11.5$	$G_3 = 3.3$	$v_3 = 0.3$	

To perform a structural analysis of the implant after topological optimization, the stem was redesigned through SolidWorks; in addition, the femoral head, the PMMA cement coating and a section of the femur bone were designed to provide support for the implant. These were applied as a boundary condition, as seen in Figure 4. The same critical loading conditions as those used in the previous section were used on the femoral head; instead, the fixed support condition was applied to the femoral bone base.

2.5. Finite Element Simulation of the Femoral Stem Forging Process

To carry out the simulation of the process of forging the femoral stem, the variables that affect the moment of forging were determined: the pressing speed, the temperature of the piece, and the properties of the materials of both the piece to be forged and the press.

Mesh Generation, Load Application and Boundary Conditions for Forging Process

First, models of the preformed part of the titanium stem and the tungsten press were designed using SolidWorks software, and then these models were transferred to the ANSYS program for dynamic analysis. Figure 5 presents the preformed femoral stem; this piece is made through prior machining to reduce the work in forging.

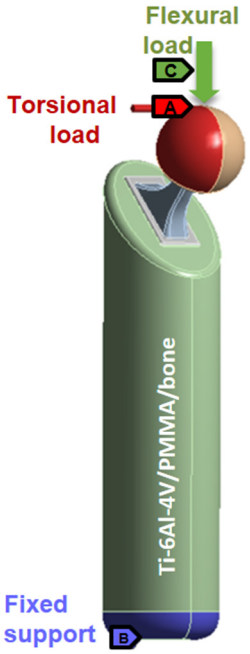

Figure 4. Load distribution for structural analysis.

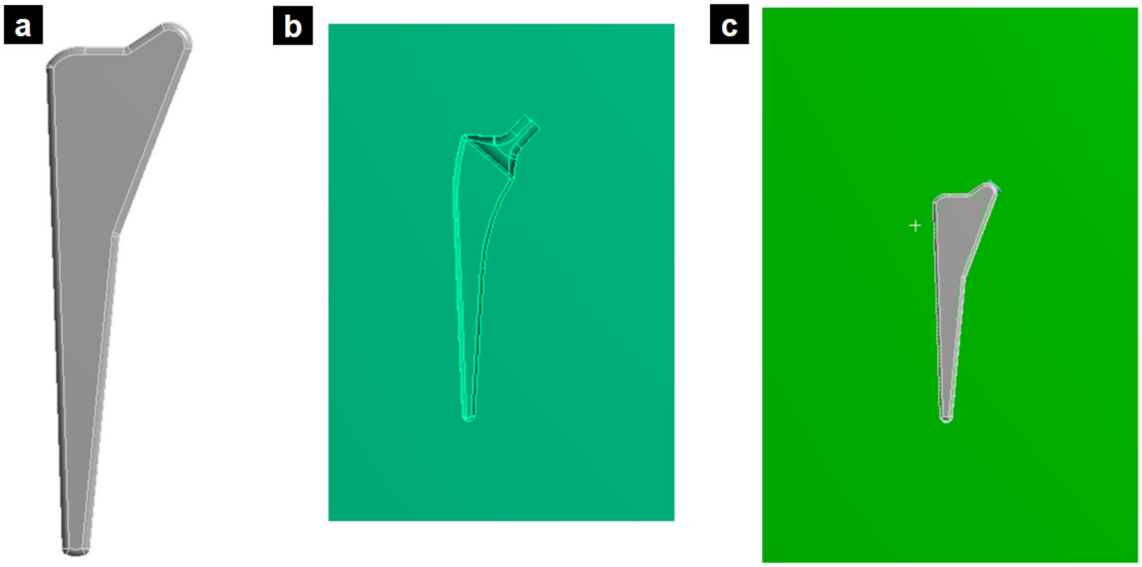

Figure 5. (**a**) Preformed piece of the TI-6Al-4V femoral stem, (**b**) tungsten press, and (**c**) preformed piece on the press.

In addition, the complexity of the design of the final femoral stem was reduced; the press molds did not present a design with very narrow curves in order to reduce the complexity of the model in the simulation and reduce the simulation times.

For the dynamic analysis, one of the molds of the tungsten carbide press was fixed, while the displacement was applied on the upper die. Initially, the molds were separated by a distance of 15 mm and the initial titanium working part for the preforming stage was 14 mm in thickness (Figure 5c). To study the temperature of the forging process, the process was analyzed from 700 °C to 900 °C, and the pressing speed was simulated at 0.14 m/s, 0.75 m/s, 1 m/s, 1.4 m/s and 2.8 m/s. The contact between the molds and the piece was made frictionless to simplify the model and convergence. The material of the press was a tungsten carbide (Table 6), and the stem was simulated with validated properties and the model constants of Ti-6Al-4V obtained in a previous work by Tuninetti et al. [24–27], as given in Tables 1–3.

Table 6. Mechanical properties of tungsten carbide press [31].

Tungsten Alloy	Value
Modulus of elasticity (GPa)	700
Melting point (°C)	3410
Density (kg/m^3)	17,000
Poisson's ratio	0.31
Compressive yield stress and ultimate stress	1.4 GPa/2.7 GPa

3. Results and Discussions

3.1. Shape Optimization of Femoral Implant

The novel implant design was generated using topological optimization, resulting in a 26% reduction in mass compared to the standard design. This mass reduction was strategically achieved by lightening areas of the implant experiencing lower stress levels, as identified through the optimization process. Importantly, this reduction was carefully managed to maintain the essential mechanical functionalities of the prosthesis. However, while topological optimization can achieve a mass reduction in the implant design, it is crucial to consider the overall impact on the biomechanical performance. Simply being lighter does not guarantee superiority over other solutions. A comprehensive evaluation should compare this approach to alternative designs, including anatomically fitted implants, to determine the optimal balance of weight, stress distribution, and long-term clinical outcomes.

Figure 6 illustrates the redesigned femoral stem, showcasing the section where material was removed based on the topological optimization results. Finite element analysis confirmed that this mass reduction did not significantly impact the prosthesis's mechanical performance.

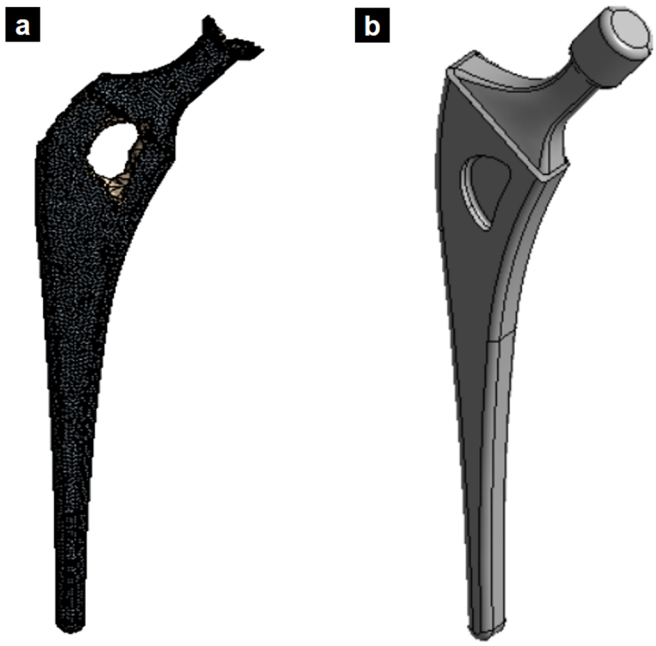

Figure 6. (**a**) Topological optimized femoral stem. (**b**) New design of titanium alloy femoral stem based on the applied topology optimization.

3.2. Numerical Results of the Computational Structural Analysis

In the structural analysis of the femoral implant, various simulations were carried out, where an element size of 2, 3 or 5 mm was iterated. Table 7 provides a summary of the structural analysis of the stem bone at different mesh sizes.

Table 7. Structural analysis of the stem at different element sizes.

Meshing, Element Size	Displacement (mm)	Equivalent Stress (MPA)	Equivalent Strain
2 mm	1.326	724.5	0.006647
3 mm	1.325	715.9	0.006565
5 mm	1.324	708.2	0.006501

The model of the topologically optimized femoral implant is attached to the modeled bone by PMMA cement (properties in Table 5). Upon the application of operational loads, the greatest displacement occurs in the section of the femoral head, where the implant is subjected to loads produced by the body movement of the patient (Figure 7). This region, in contrast to the stable stem base, exhibited displacement ranging from 1.32–0.01 mm. This minimum displacement between the base of the stem and the head indicates the stability of the stem joint.

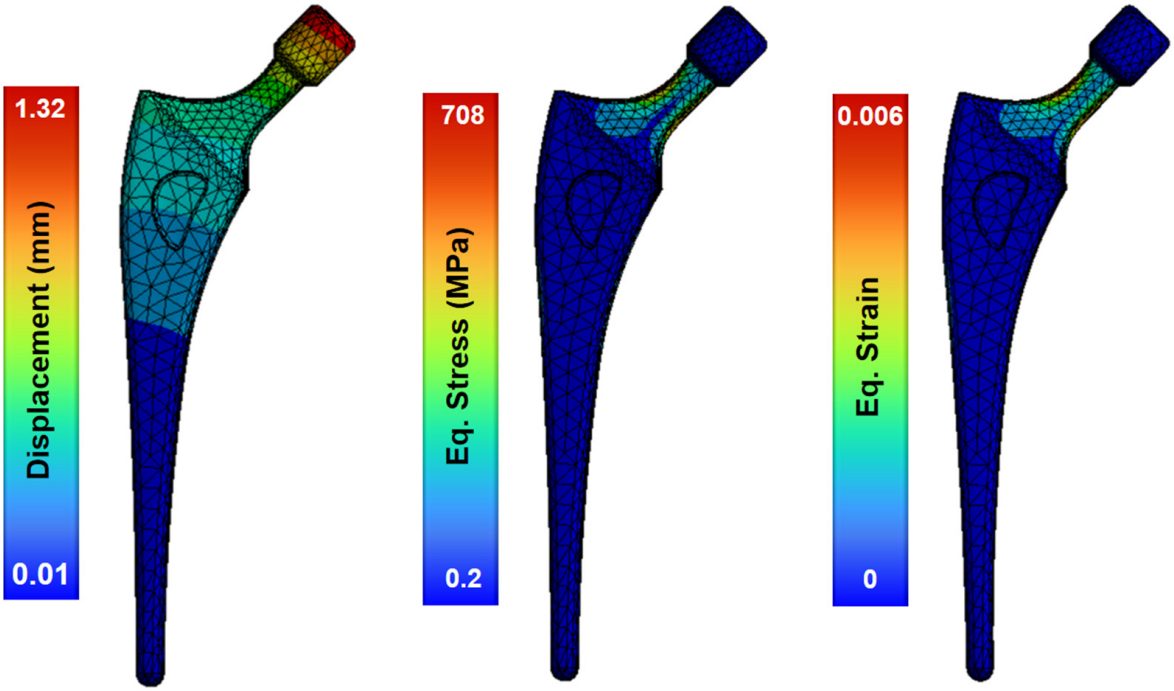

Figure 7. Structural analysis of the femoral stem showing the field of deformations, strains and stresses.

The maximum stress occurs in the femoral neck of the stem, produced by the bending generated by the loads applied to the femoral head. The maximum stress reached 708 MPa, a stress level more than acceptable for the material, as the yield strength of Ti-6Al-4V alloy is close to 920 MPa. This maximum stress is concentrated in the areas that have a reduced section like the neck of the stem, with the stress values ranging between 80 MPa and 300 MPa (Figure 7). Because the yield strength of Ti-6Al-4V alloy is 1100 MPa, it can be assumed that the implant design has no critical issues. The maximum equivalent strain occurs at the neck of the femoral stem with 0.6%, and the maximum value of total deformation is 1.3 mm in the femoral head. This femoral model shows a low stiffness and provides a uniform strain distribution, which is advantageous for mitigating stress shielding.

3.3. Forming Simulation of the Femoral Implant and Current Limitations for Future Directions

Developing forging methods for medical implant components is essential to improve properties such as the fracture toughness, strength, microstructure, and biocompatibility, ensuring better performance and durability for successful medical procedures [32]. Research in the literature on the forging of femur stems is currently scarce.

In this study, an analysis of the forging process was performed using numerous finite-element-based large deformation simulations, reaching strain levels only for the pre-forming process. Figure 8 shows the preforming results in one stage at 800 °C and a speed of 1.4 m/s, with non-uniform deformation producing local zones of equivalent stress with a maximum value of 1050 MPa and a displacement of 2.21 mm.

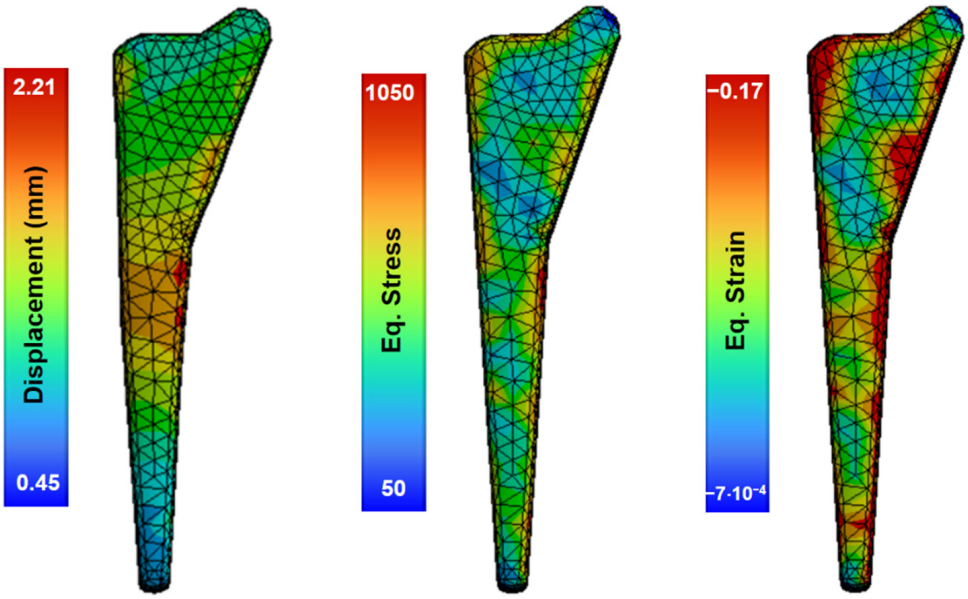

Figure 8. Simulations of the forging process of the material at 800 °C and die speed of 1.4 m/s.

At this current stage, large simulations of the final femur implant shape require several improvements and further research to achieve accurate results. In this regard, the following strategies are recommended. As the speeds of the forging process were low compared to the general simulations of explicit dynamics, a quasi-static model that does not include material dynamics or inertia forces in the implementation could be used. Lagamine numerical tools including the Norton–Hoff model could be a good option; however, this model requires the implementation of coupled damage for different temperatures or the use of non-coupled fracture criteria. In addition, the inherent complexities in the plasticity and damage modelling of processes with large plastic deformations and the effects of friction, element distortion, velocity and temperature variations should be carefully set and verified. The complexity of the model includes not only elastoplastic material laws, but also fracture laws through deactivation elements. Other commercially available software, such as Abacus, could also be tested for the optimization of this manufacturing process.

4. Conclusions

This study focused on the shape optimization of femoral hip prostheses using finite element modeling in order to reduce the weight and material usage. The static analysis of the optimized femoral stem under an operational load included the interactions with PMMA and the femoral bone.

The resulting maximum local stress of 708 MPA after the mesh sensitivity analysis occurred in the femoral neck of the stem, confirming the acceptable strength of the Ti-6Al-4V and that the proposed design had no critical issues.

A high stress gradient occurred in concentrated areas with a reduced section, such as the neck range between 80 MPa and the maximum local stress, with an average value of about 300 MPa.

The maximum equivalent strain occurs at the neck of the femoral stem with 0.6%, and the maximum value of total deformation is 1.3 mm in the femoral head.

This femoral model shows low stiffness and provides a uniform strain distribution, which is advantageous for mitigating stress shielding.

Topological optimization can reduce the implant mass, but the overall impact on biomechanical performance must be considered. Simply being lighter does not ensure superiority over other designs. A comprehensive evaluation comparing this approach to alternatives, such as anatomically fitted implants, is needed to determine the optimal balance of weight, stress distribution, and long-term outcomes.

Investigating the finite-element-based process of forging a femoral stem through dynamic analysis was challenging. The temperature and punching speed conditions were studied in different forging processes of a femoral stem. The literature states that the ideal speed in the forging process is between 5 mm/s and 30 mm/s; however, further research is required to investigate the optimized forging speed and optimal temperatures of the alloy under superplasticity to avoid cracking and to ensure an accurate final shape.

Finally, as demonstrated by previous studies, we confirmed that failures in the femur bone joint may be avoided by the optimization of the design using results from FEA analysis [33]. However, the results from simulations must be experimentally verified in order to ensure accuracy. The lack of validation may limit the reliability of the results obtained through the FEA. Current study is limited to static loadings, and for fatigue analysis or dynamic behavior, the reader is directed to ref. [34].

To verify the accuracy of finite element simulations and ensure the long-term performance of the optimized and tailored femoral implants, extensive biomechanical testing in a simulated physiological environment is required. Research should consider the use of the investigated alloy and materials, the respective manufacturing process, the use of cadaveric or synthetic bone specimens, and the reproduction of the intended surgical procedure. Physiological loading patterns could be applied and experiments in a temperature- and fluid-controlled environment could be performed to determine implant stability, the stress distribution and bone–implant interactions. Measurement techniques should include strain gauges, digital image correlation and computed microtomography to quantitatively and qualitatively compare experimental data with simulation predictions. Investigating the biomechanical compatibility of the proposed implant design will require ethical approvals, a correct definition of the sample size and possible statistical analysis.

Author Contributions: Conceptualization, V.T.; methodology, V.T. and G.F.; validation, G.F. and V.T.; formal analysis, G.F., V.T., A.O., S.N., D.C., C.G.-H., B.M., C.G., G.P. and R.V.; investigation, G.F.; resources, V.T. and R.V.; writing—original draft preparation, G.F. and V.T.; writing—review and editing, S.N., B.M., G.P., A.O., D.C., C.G.-H., C.G., R.V. and V.T.; visualization, G.F.; supervision, V.T. All authors have read and agreed to the published version of the manuscript.

Funding: This research received no external funding.

Institutional Review Board Statement: Not applicable.

Informed Consent Statement: Not applicable.

Data Availability Statement: The raw data supporting the conclusions of this article will be made available by the authors upon request.

Conflicts of Interest: The authors declare no conflicts of interest.

Nomenclature

A	Initial yield stress of the material.
B	Hardening coefficient.
C	Constant strain rate.
D	Damage.
m	Softening exponent.
n	Strain hardening exponent.
$\overline{\sigma}$	Yield stress
ε_p	Plastic deformation
$\dot{\varepsilon}$	Plastic deformation rate
$\dot{\varepsilon}_0$	Reference plastic deformation rate
ε_D	Plastic deformation equivalent to the onset of damage
d_1	Johnson–Cook damage constant
d_2	Johnson–Cook damage constant
d_3	Johnson–Cook damage constant
d_4	Johnson–Cook damage constant
d_5	Johnson–Cook damage constant

References

1. Zheng, Z.; Chen, S.; Liu, X.; Wang, Y.; Bian, Y.; Feng, B.; Zhao, R.; Qiu, Z.; Sun, Y.; Zhang, H.; et al. A bioactive polymethylmethacrylate bone cement for prosthesis fixation in osteoporotic hip replacement surgery. *Mater. Des.* **2021**, *209*, 109966. [CrossRef]
2. Maggs, J.; Wilson, M. The Relative Merits of Cemented and Uncemented Prostheses in Total Hip Arthroplasty. *Indian J. Orthop.* **2017**, *51*, 377–385. [CrossRef]
3. Niinomi, M. Recent research and development in titanium alloys for biomedical applications and healthcare goods. *Sci. Technol. Adv. Mater.* **2003**, *4*, 445–454. [CrossRef]
4. Sarraf, M.; Rezvani Ghomi, E.; Alipour, S.; Ramakrishna, S.; Liana Sukiman, N. A state-of-the-art review of the fabrication and characteristics of titanium and its alloys for biomedical applications. *Bio-Design Manuf.* **2022**, *5*, 371–395. [CrossRef] [PubMed]
5. Zhang, L.; Chen, L. A Review on Biomedical Titanium Alloys: Recent Progress and Prospect. *Adv. Eng. Mater.* **2019**, *21*, 1801215. [CrossRef]
6. Yang, R.; Hao, Y.; Li, S. Development and Application of Low-Modulus Biomedical Titanium Alloy Ti2448. In *Biomedical Engineering, Trends in Materials Science*; Laskovski, A.N., Ed.; InTech: Rijeka, Croatia, 2011.
7. Kumar, P.; Jain, N.K. Finite element analysis of femoral prosthesis using Ti-6Al-4 V alloy and TiNbZrTaFe high entropy alloy. *Mater. Today Proc.* **2021**, *44*, 1195–1201. [CrossRef]
8. Ceddia, M.; Solarino, G.; Giannini, G.; De Giosa, G.; Tucci, M.; Trentadue, B. A Finite Element Analysis Study of Influence of Femoral Stem Material in Stress Shielding in a Model of Uncemented Total Hip Arthroplasty: Ti-6Al-4V versus Carbon Fibre-Reinforced PEEK Composite. *J. Compos. Sci.* **2024**, *8*, 254. [CrossRef]
9. Todo, M.; Fukuoka, K. Biomechanical Analysis of Femur with THA and RHA implants using CT-Image Based Finite Element Method. *J. Orthop. Sport Med.* **2020**, *2*, 89–107. [CrossRef]
10. Naghavi, S.A.; Tamaddon, M.; Garcia-Souto, P.; Moazen, M.; Taylor, S.; Hua, J.; Liu, C. A novel hybrid design and modelling of a customised graded Ti-6Al-4V porous hip implant to reduce stress-shielding: An experimental and numerical analysis. *Front. Bioeng. Biotechnol.* **2023**, *11*, 1092361. [CrossRef]
11. Johnson, J.E.; Brouillette, M.J.; Miller, B.J.; Goetz, J.E. Finite Element Model-Computed Mechanical Behavior of Femurs with Metastatic Disease Varies between Physiologic and Idealized Loading Simulations. *Biomed. Eng. Comput. Biol.* **2023**, *14*, 11795972231166240. [CrossRef]
12. Fraldi, M.; Esposito, L.; Perrella, G.; Cutolo, A.; Cowin, S.C. Topological optimization in hip prosthesis design. *Biomech. Model. Mechanobiol.* **2010**, *9*, 389–402. [CrossRef] [PubMed]
13. Rostamian, R.; Silani, M.; Ziaei-Rad, S.; Busse, B.; Qwamizadeh, M.; Rabczuk, T. A finite element study on femoral locking compression plate design using genetic optimization method. *J. Mech. Behav. Biomed. Mater.* **2022**, *131*, 105202. [CrossRef] [PubMed]
14. Tan, C.; Zou, J.; Li, S.; Jamshidi, P.; Abena, A.; Forsey, A.; Moat, R.J.; Essa, K.; Wang, M.; Zhou, K.; et al. Additive manufacturing of bio-inspired multi-scale hierarchically strengthened lattice structures. *Int. J. Mach. Tools Manuf.* **2021**, *167*, 103764. [CrossRef]
15. Ceddia, M.; Solarino, G.; Cassano, G.D.; Trentadue, B. Finite Element Study on Stability in the Femoral Neck and Head Connection to Varying Geometric Parameters with the Relates Implications on the Effect of Wear. *J. Compos. Sci.* **2023**, *7*, 387. [CrossRef]
16. Meena, V.K.; Kumar, M.; Pundir, A.; Singh, S.; Goni, V.; Kalra, P.; Sinha, R.K. Musculoskeletal-based finite element analysis of femur after total hip replacement. *Proc. Inst. Mech. Eng. Part H J. Eng. Med.* **2016**, *230*, 553–560. [CrossRef]
17. Oza, A.D.; Gupta, N.; Singh, R. Design and non-linear finite element analysis of titanium-based femoral hip-stem for Indian population. *Int. J. Interact. Des. Manuf.* **2023**, *17*, 2489–2493. [CrossRef]

18. Kebbach, M.; Soodmand, I.; Krueger, S.; Grupp, T.M.; Woernle, C.; Bader, R. Biomechanical assessment of mobile-bearing total knee endoprostheses using musculoskeletal simulation. *Appl. Sci.* **2022**, *12*, 182. [CrossRef]
19. Xiao, Z.; Wu, L.; Wu, W.; Tang, R.; Dai, J.; Zhu, D. Multi-Scale Topology Optimization of Femoral Stem Structure Subject to Stress Shielding Reduce. *Materials* **2023**, *16*, 3151. [CrossRef]
20. Kang, Y.; Kim, S.; Kim, J.; Lee, J.W.; Park, J.C. Evaluating the validity of lightweight talar replacement designs: Rational models and topologically optimized models. *Biomater. Res.* **2022**, *26*, 10. [CrossRef]
21. Sun, X.; Curreli, C.; Viceconti, M. Finite Element Models to Predict the Risk of Aseptic Loosening in Cementless Femoral Stems: A Literature Review. *Appl. Sci.* **2024**, *14*, 3200. [CrossRef]
22. Neto, M.A.; Paulino, M.F.; Amaro, A.M. Effect of Plate Configuration in the Primary Stability of Osteotomies and Biological Reconstructions of Femoral Defects: Finite-Element Study. *Bioengineering* **2024**, *11*, 416. [CrossRef] [PubMed]
23. Gil, F.J.; Planell, J.A. Aplicaciones biomédicas del titanio v sus aleaciones. *Biomecánica* **1993**, *1*, 34–42. [CrossRef]
24. Tuninetti, V.; Forcael, D.; Valenzuela, M.; Martínez, A.; Ávila, A.; Medina, C.; Pincheira, G.; Salas, A.; Oñate, A.; Duchêne, L. Assessing Feed-Forward Backpropagation Artificial Neural Networks for Strain-Rate-Sensitive Mechanical Modeling. *Materials* **2024**, *17*, 317. [CrossRef] [PubMed]
25. Sepúlveda, H.; Valle, R.; Pincheira, G.; Prasad, C.S.; Salas, A.; Medina, C.; Tuninetti, V. Dynamic numerical prediction of plasticity and damage in a turbofan blade containment test. *Proc. Inst. Mech. Eng. Part L J. Mater. Des. Appl.* **2023**, *237*, 2551–2560. [CrossRef]
26. Tuninetti, V.; Sepúlveda, H. Computational Mechanics for Turbofan Engine Blade Containment Testing: Fan Case Design and Blade Impact Dynamics by Finite Element Simulations. *Aerospace* **2024**, *11*, 333. [CrossRef]
27. Tuninetti, V.; Sepúlveda, H.; Beecher, C.; Rojas-Ulloa, C.; Oñate, A.; Medina, C.; Valenzuela, M. A Combined Experimental and Numerical Calibration Approach for Modeling the Performance of Aerospace-Grade Titanium Alloy Products. *Aerospace* **2024**, *11*, 285. [CrossRef]
28. Cilingir, A.C.; Ucar, V.; Kazan, R. Three-dimensional anatomic finite element modelling of hemi-arthroplasty of human hip joint. *Trends Biomater. Artif. Organs* **2007**, *21*, 63–72.
29. Morán, D.; Navarro, N.; García, N.; Caballero, R. Biomecánica de la prótesis total de cadera cementada y no cementada. *Canar. Médica Y Quirúrgica* **2011**, *25*, 32–48.
30. Krone, R.; Schuster, P. *An Investigation on the Importance of Material Anisotropy in Finite-Element Modeling of the Human Femur*; SAE Technical Paper: Detroit, MI, USA, 2006.
31. Shabalin, I.L. Tungsten Carbides. In *Ultra-High Temperature Materials IV*; Springer International Publishing: Cham, Switzerland, 2022; pp. 11–829. ISBN 978-3-031-07175-1.
32. Turner, R.; Antonic, J.; Warnken, N. 3D Forging Simulation of a Multi-Partitioned Titanium Alloy Billet for a Medical Implant. *J. Manuf. Mater. Process.* **2019**, *3*, 69. [CrossRef]
33. Belwanshi, M.; Jayaswal, P.; Aherwar, A. A study on finite element analysis methodologies and approaches used for total hip arthroplasty. *Mater. Today Proc.* **2022**, *56*, 2596–2604. [CrossRef]
34. Balasubramani, V.; Gokul, D.; Gokul, R.K. Modelling and finite element analysis of fractured femur bone with locking compression plate under fatigue load condition. *Mater. Today Proc.* 2023, *in press*. [CrossRef]